Testing and modeling liquefying fuel combustion in hybrid propulsion

Alexandra Weinstein and Alon Gany
Faculty of Aerospace Engineering, Technion – Israel Institute of Technology
Haifa 32000, Israel

Abstract

Hybrid motors are considered an alternative for space launchers due to their safety and high energetic performance. Nevertheless, classical hybrid combustors employing polymeric fuels are characterized by a low fuel regression rate resulting in low thrust levels that may not be adequate. The present research presents experimental investigation and theoretical model of liquefying (paraffin-based) fuels, featuring high regression rates. The model developed includes an additional feature and mass loss mechanism, i.e., the liquid melt flowing along the grain. The test results exhibit a good correlation with the model predictions.

1. Introduction

Hybrid motors consist of fuel and oxidizer components in different physical states. Polymeric material is typically used as a solid fuel. It is placed in the combustion chamber as a hollow-cylinder grain with a single port or multiple ports. Oxidizer can be chosen from a variety of oxidizer used in liquid rocket engines. It is injected into the fuel port(s) in a liquid or gaseous form. The combustion occurs in the gas phase within the boundary layer over the surface of the solid fuel grain. Often, the combustion chamber includes an aft-mixing-chamber to allow the completion of the chemical reaction. Overview and history of hybrid propulsion are presented by Altman and Holtzman [1].

Energetic performances of hybrid motors are comparable to liquid rockets and better than solid rockets due to the use of more energetic liquid oxidizers. Compared to liquid rockets hybrid systems can provide simple capabilities of throttling (via control of only the oxidizer flow rate) as well as shutdown and on/off operations. It might be significant for precise orbit insertion or space operation.

The phase separation between the fuel and the oxidizer increases safety during motor development and operation since no explosion or major fire can occur upon accidental contact between the fuel and oxidizer. In addition, hybrid motor operation is insensitive to cracks or defects in the fuel grain, since fuel regression rate is related to the oxidizer flow rate and to the heat flux from the bulk flow to the surface. Another significant advantage of hybrid motors is the option of a "green" propellant combination of minimum environmental impact.

The most significant potential use of hybrid motors is for large launch boosters. The combination of safety, "green" propellant system, and high energetic performance (especially when using liquid oxygen (LOX) as the oxidizer), is particularly attractive.

Hybrid systems are characterized by a low fuel regression rate, typically an order of magnitude lower than that of common solid propellants. For many potential applications, particularly for space launch boosters that require high thrust levels, it is a major drawback. This has motivated search for high burning rate fuels.

1.1 New Trend of Enhancing Fuel Regression Rate

As mentioned above, different applications of hybrid motors, particularly for space launchers, require high thrust, which imply higher overall fuel consumption rates. To avoid the complex multi-port grain configuration, a new direction has been proposed and investigated in recent years: the use of high burning rate, liquefying fuels, mostly paraffin-based fuels.

A most comprehensive experimental and theoretical work on paraffin fuels has been conducted at Stanford University by Karabeyoglu at al. [2-6]. They suggested that the most efficient way to increase burning rate of hybrid systems is to use a fuel that will generate mass transfer by mechanical means in addition to the mass transfer by gasification of the fuel. For materials forming a low viscosity liquid layer on the surface during their combustion, the mechanical mass transfer takes place by droplets entrainment into the gas stream

The hybrid diffusion flame theory was generalized to hybrid fuels that burn by forming a liquid layer. It was shown that the relatively thick layer formed may be unstable under hybrid operating conditions. Several additional works that have been conducted in different universities are summarized by Gany and Lazarev [7].

2. Experimental

2.1 Experimental Setup

The laboratory scale static firing test setup includes motor (combustion chamber), test stand, gaseous oxygen tank, measuring gauges for thrust, pressure, and flow rate, and computerized data acquisition and control system. The combustion chamber has a single-port, 21mm initial diameter and 190 mm long. At the aft end of the combustor there is a water-cooled mixing chamber, 42mm internal diameter and 120mm long. A choked converging (only) motor nozzle has been used in the experiments. Motor ignition is accomplished by introducing a small amount of ethylene gas for a short time at the beginning of the test, and igniting by a spark plug. Gaseous oxygen has been used as oxidizer. Oxygen flow rate is controlled and measured by a replaceable choked nozzle in the oxygen supply line. The present configuration allows oxygen flow rate up to about 40 g/s, yielding oxygen mass flux as high as $10\,g/s\,cm^2$.
The combustion chamber pressure can be roughly estimated before the test by selecting the exit nozzle dimensions**.**
The setup used in the present research is presented in Figure 1.

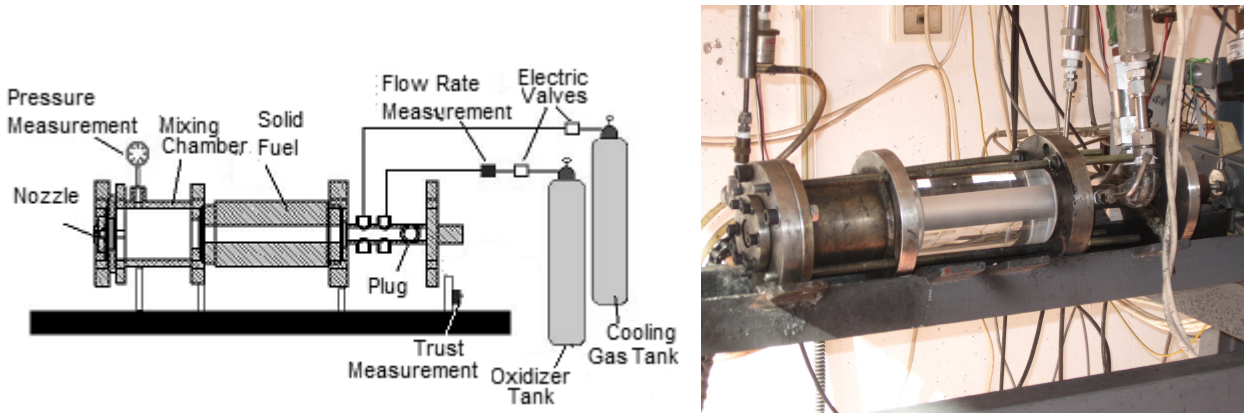

Figure 1: Schematic and picture of test setup

The paraffin used for the investigation was MW-704, with melting point of $70-74\ ^{\circ}C$ and density of $0.747\ g/cm^3$.
The test motors were prepared by casting molten paraffin into vertically positioned motor case. The port was created by placing a cylindrical pin along the centerline of the motor during casting. Paraffin fuel tends to shrink during cooling and solidifying, so at the end of the process additional molten paraffin was added to the grain. There were no gaps between the paraffin layers since hot paraffin melted the adjacent cooler layer and there was a good gluing between the layers. Also no gap was noticed between the paraffin and the motor case.
Since fuel regression rate is related to the oxidizer flow rate, it was difficult to reach high O/F ratio by merely increasing the oxidizer flow rate. In order to reach higher levels of the O/F ratio it was decided to use shorter fuel grains while keeping the high oxidizer flow rate. Both 95 mm long and 63 mm grains (a half and a third of the original grain length, respectively) were used.
Pressure output of a typical test is shown in Figure 2. The burning time of each firing test was 6-8 sec which is long enough to assume fully developed combustion while keeping small enough changes in internal diameter of the grain for using average values.

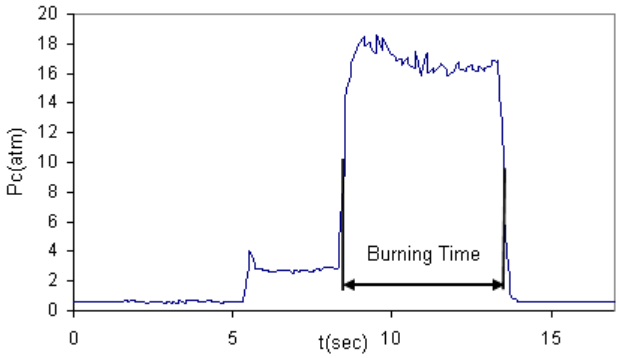

Figure 2: Typical static firing test output

After initial firing tests with plain paraffin, it became obvious that plain paraffin exhibits poor mechanical properties and undergoes severe melting especially at low flow rates. Some unburned fuel may leave the combustion chamber in the form of drops and burn outside. In addition at lower oxidizer fluxes certain amount of unburned fuel was found inside the aft-chamber.

2.2 Results

The fuel burning rate is an important parameter in the internal ballistics and overall performance of hybrid motors. The average regression rate was calculated from mass loss and burning time. Figure 3 presents the dependence of the burning rate of pure paraffin on oxidizer mass flux. The burning rate of the plain paraffin obtained in the current research was about 5 times higher than that of the classic polymeric hybrid fuels.
The results are compared to the regression rate data of polymeric fuel obtained from a series of experiments conducted on the same experimental setup as the paraffin fuel. Power curve fit for each fuel is plotted to show the regression rate trend. The results are also compared to the experimental results obtained in Stanford [5] and to an HTPB regression rate line [8].

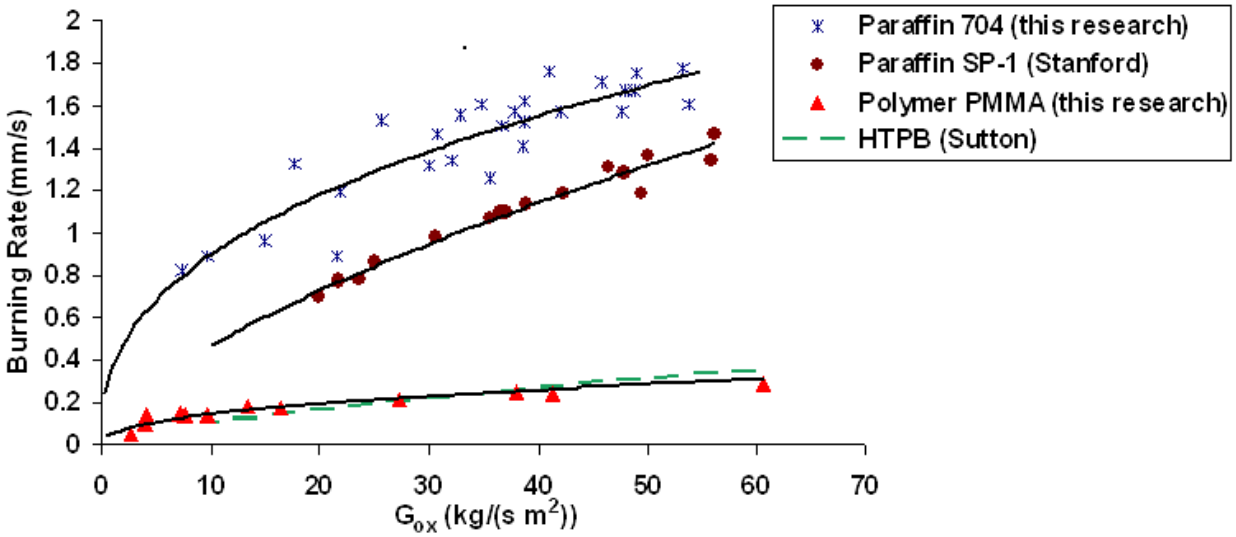

Figure 3: Comparisson of experimental regression rate of different fuels

The regression rate correlation obtained from the experimental data for the plain paraffin is:

$$\dot{r} = 0.36 G_{OX}^{0.40} \quad \textbf{(1)}$$

where $\dot{r}$ is time and space averaged regression rate of the fuel in mm/s and G_{OX} is the average oxidizer mass flux in $kg/\left(s\ m^2\right)$.

Average fuel regression rate $\dot{r}$ calculation is based on the overall fuel mass loss during the firing test, and oxidizer flow rate is calculated from the oxidizer flow rate $\dot{m}_{ox}$ and average motor diameter.

$$G_{ox} = \frac{8\dot{m}_{ox}}{\pi\left(d_i^2 + d_f^2\right)} \quad \textbf{(2)}$$

Figure 4 presents delivered C* values of plain paraffin obtained from experimental measurements compared to theoretical calculations obtained from thermochemical program PEP plotted vs. O/F ratio. Most of the test results exhibit C* efficiency of 90%-95%, though a few yield values of 80%-85%.

Plain paraffin undergoes severe melting resulting in generation of quite a thick molten layer. This process may result in some unburned fuel leaving the combustion chamber in the form of droplets and burning outside. It is indicated by a very large exhaust flame observed during motor firing. In addition at lower oxidizer fluxes certain amount of unburned fuel was found inside the aft-chamber. It was collected, weighted and added to the grain mass after combustion for performance and efficiency calculations. The ejection of some unburned fuel droplets lowers the actual C* and combustion efficiency.

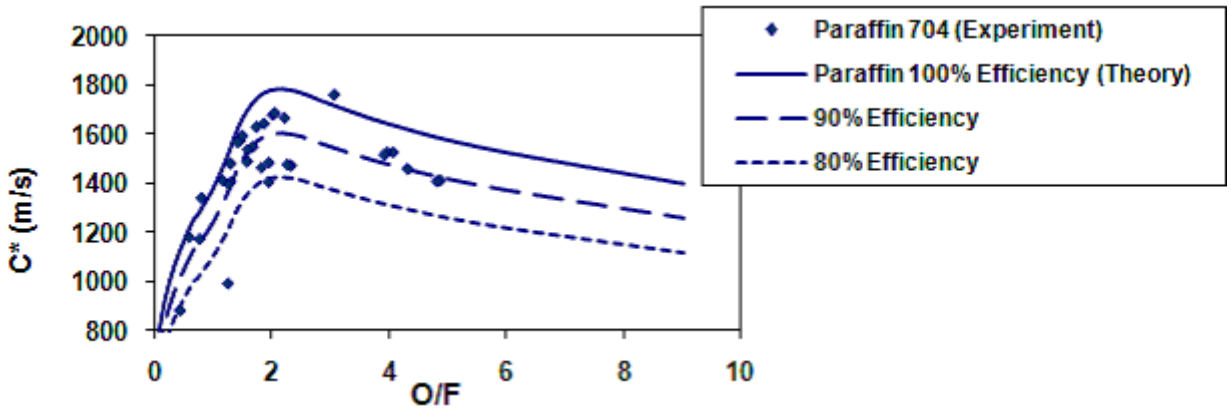

Figure 4: C* vs. O/F for plain paraffin

3. Theoretical Model

The goal of the currently developed model is to be able to predict the overall regression rate and liquid layer thickness of the paraffin based fuel. In addition, the model includes and evaluates the contribution of a mechanism that has not been accounted for in other models: the flow of a molten material along the solid surface, its characteristics (e.g., velocity, thickness), and its role in the overall fuel mass transfer phenomena.

Classical hybrid combustion is characterized by a gas-phase diffusion flame established within the boundary layer over the burning solid fuel surface. Gaseous oxidizer diffuses from the core flow towards the flame location, whereas fuel gases resulting from the gasifying condensed fuel surface diffuse towards the flame sheet from the opposite direction. Marxman and colleagues [9], [10], [11] conducted detailed modeling of the hybrid combustion in the 1960's and early 1970's. Their initial simplified model assumes an infinitely fast chemical reaction forming an infinitesimally thin diffusion flame sheet, where oxidizer and fuel fluxes meet at a stochiometric ratio. In addition Reynolds analogy was used assuming similarity between momentum and sensible enthalpy boundary layers (i.e.,

similarity between axial velocity and temperature) at least throughout the range from the condensed fuel surface to the flame sheet.
The process of the paraffin based hybrid fuel combustion occurs in a three phase environment: solid, liquid and gas. As the fuel reaches the melting point, a thin liquid layer forms on its surface. The liquid (melt) layer heats up, reaching the evaporation point at the interface with the gas phase. The gasifying fuel enters the core flow and feeds the gas phase diffusion flame at some distance from the condensed surface. The melting and the evaporation are caused by heat transfer from the flame to the surface of the fuel mainly by forced convection (and to a much less extent by radiation). The liquid and solid layers are heated by heat conduction and some radiation (in case of a transparent material).
It was assumed that the high regression rate of the paraffin based fuel cannot be a result only of vaporization process and that additional mechanisms of the fuel mass loss take part in the process. Karabeyoglu at al. [3], [4] suggested a mechanism of entrainment. Liquid fuel drops are torn from the liquid layer by the shear stress caused by the turbulent gas flow over the liquid layer, and enter the gaseous free stream. They conducted a comprehensive work on entrainment process and liquid layer stability in liquefying hybrid fuels.
As mentioned before, in the present research we discuss and investigate the characteristics and contribution to the overall mass loss of an additional mechanism resulting from a possible flow of the liquid layer along the surface. Such flow is implied from the shear stress applied by the gas flow over the liquid layer. This mechanism has been implemented in the current model. A similar mechanism for the combustion of metals in high shearing regime involving melting was described by Gany and Caveny [12].
Schematic of the heat and mass transfer in the different phases of the fuel is shown in Figure 5.
The initial development of the model including heat transfer balance and description of different mechanisms and fuel properties can be found in previous work by the authors [13].
Regression rates for the mechanisms of melting, vaporization and entrainment can be found from the heat transfer balances on the gas-liquid and liquid-solid interfaces. Radiation was neglected in the calculations.
Heat transfer balance on the gas-liquid interface is:

$$q_{conv} = q_{cond,l} + q_v \tag{3}$$

where q_{conv} is the heat transfer from the flame to the surface (the interface between the gas and melt layer) by convection, given by:

$$q_{conv} = h\left(T_c - T_v\right) \tag{4}$$

where h is convection coefficient, T_c is combustion temperature and T_v is the paraffin evaporation temperature.

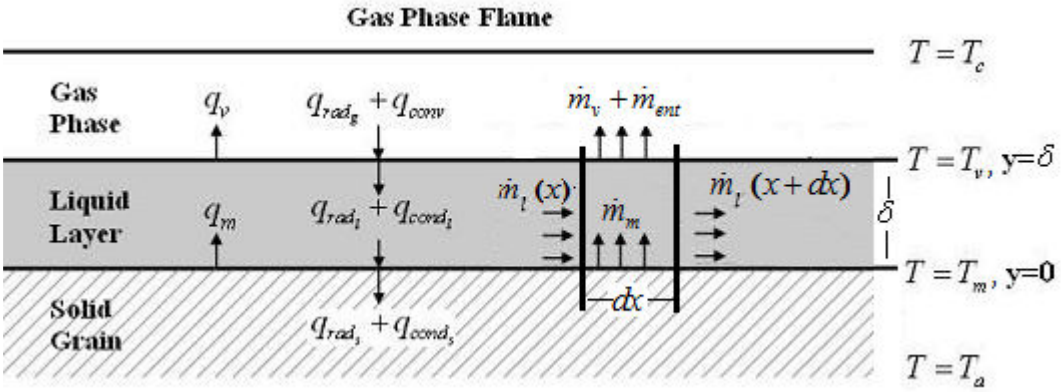

Figure 5: Schematic of heat and mass transfer

$q_{cond,l}$ is heat transferred by conduction into the liquid layer. The liquid layer is thin enough to assume linear temperature profile through it. Under the boundary conditions, the temperature at the liquid-gas interface is the

paraffin evaporation temperature, and the temperature at the liquid-solid interface is the paraffin melting point. We can then state that:

$$q_{cond_l} = k_l \frac{\Delta T}{\Delta y} = k_l \frac{T_v - T_m}{\delta} \quad \textbf{(5)}$$

where k_l is conduction coefficient of the liquid, T_m is melting temperature of the solid paraffin and δ is the thickness of the melt layer.
q_v is heat of evaporation:

$$q_v = \rho_l \dot{r}_v \left(H_v + C_{p,l} \left(T_v - T_m \right) \right) \quad \textbf{(6)}$$

where ρ_l is the density of the molten liquid, $\dot{r}_v$ rate of vaporization of liquid at liquid-gas interface, H_v enthalpy of vaporization, $C_{p,l}$ specific heat of the liquid and T_m is melting temperature of the solid grain.
Heat transfer balance on the liquid-solid interface is:

$$q_{cond,l} = q_{cond,s} + q_m \quad \textbf{(7)}$$

where the heat conduction through the solid grain is given by:

$$q_{cond,s} = k_s \left. \frac{dT_s}{dy} \right|_{y=0} \quad \textbf{(8)}$$

and heat of melting q_m is

$$q_m = \rho_s \dot{r}_m \left(H_m + C_{p,s} \left(T_m - T_a \right) \right) \quad \textbf{(9)}$$

where ρ_s is the density of the solid fuel, $\dot{r}_m$ is the melting rate, H_m enthalpy of melting, $C_{p,s}$ specific heat of the solid and T_a is the temperature deep within the grain (typically the ambient temperature).
The rate of entrainment of the liquid drops into the gas stream, suggested by Karabeyoglu et al. [3] is

$$\dot{r}_{ent} = a \frac{G^{2\alpha}}{\dot{r}^{\beta}} \quad \textbf{(10)}$$

where: $a = 6.88 \cdot 10^{-14}\ m^9/kg^3$ (for the calculations in metric units) is an entrainment parameter for paraffin, G overall mass flux and $\dot{r}$ is overall regression rate (in our case $\dot{r} = \dot{r}_m$). $\alpha = 1.5, \beta = 2$ are parameters that are constant for the given propellant.
In the calculations the following numerical values are used:

$k_g = 0.12\ W/m\ K$, $k_s = k_l = 0.14\ W/m\ K$, $H_m = 167\ J/g$, $H_v = 163\ J/g$,
$\rho_s = 747\ kg/m^3$, $\rho_l = 450\ kg/m^3$

Linear velocity profile inside the liquid layer is assumed. With no-slip condition at the gas-liquid interface, shear stress can be described as:

$$\tau_{\mathbf{i}} = \mu_g \left.\frac{\partial u_g}{\partial y}\right|_{\mathbf{i}} = \mu_l \left.\frac{\partial u_l}{\partial y}\right|_{\mathbf{i}} = \mu_l \frac{u_i}{\delta} \tag{11}$$

where $\tau_{\mathbf{i}}$ is shear stress at the interface, u_i liquid velocity at the interface $\left(u_i = u_{l,max}\right)$, and δ is the liquid layer thickness.

The net rate of melt generation up to the distance x (subtracting the fractions removed by vaporization and entrainment) should compose the flow along the surface:

$$\dot{m}_l = \pi dx\left(\dot{r}_m \rho_s - \left(\dot{r}_{ent} + \dot{r}_v\right)\rho_l\right) \tag{12}$$

where d is the motor internal diameter.

Rate of melt flowing along the surface when $u_i/2$ is the average flow velocity:

$$\dot{m}_l = \pi d\,\delta\rho_l\, u_i/2 \tag{13}$$

For steady state:

$$l\left(\dot{r}_m \rho_s - \left(\dot{r}_{ent} + \dot{r}_v\right)\rho_l\right) = \delta\rho_l\, u_i/2 \tag{14}$$

Solving equations (11) and (14) for u_i and δ yields:

$$u_i = \left(\frac{2l\tau_i}{\mu_l\rho_l}\left(\dot{r}_m \rho_s - \left(\dot{r}_{ent} + \dot{r}_v\right)\rho_l\right)\right)^{0.5} \tag{15}$$

$$\delta = \left(\frac{2\mu_l l}{\tau_i\rho_l}\left(\dot{r}_m \rho_s - \left(\dot{r}_{ent} + \dot{r}_v\right)\rho_l\right)\right)^{0.5} \tag{16}$$

Calculations were made assuming average values of regression rates at the half length of the fuel grain. Shear stress at the gas-liquid interface was calculated from the correlation for a developed turbulent boundary layer in pipes:

$$\tau_i \cong 0.0277\rho_g u_\infty \left(Re_d\right)^{-0.25} \tag{17}$$

where ρ_g is the gas density, u_∞ core stream velocity and Re_d is Reynolds number calculated for the average internal diameter of the fuel grain (i.e., port diameter) d:

$$Re_d = \frac{4\dot{m}_{tot}}{\mu_g \pi d} \tag{18}$$

where $\dot{m}_{tot}$ overall mass flow rate, μ_g gas phase viscosity.

Figure 6 presents the dependence of melt layer thickness on total mass flux predicted by the model. Calculation was made for the middle cross section along the fuel grain. One can see that the higher the flow rate, the thinner is the liquid layer. This corresponds with the observations and conclusions made from the experiments.

Figure 7 presents different regression rate mechanisms predicted by the model and normalized by the solid density to present the relative contribution of each one to the overall regression rate. Calculated results are compared to the

experimental data. The entrainment regression rate plays a more significant role in the overall regression rate as the mass flux increases. The mass loss contribution attributed to the melt flow along the surface is of the same order as the mass loss by the mechanism of entrainment. However, the higher the oxidizer flow rate the higher the mass loss due to the mechanisms of vaporization and entrainment, which makes liquid layer thinner. This observation is compatible with the trend shown in Figure 6.
The model predicts that in the range tested, the contribution of the vaporization to the overall regression rate (equal to the melting regression rate) is more significant than the contribution of the entrainment. Within the uncertainty of the different physical properties yielding an uncertainty of ±15% in the regression rate prediction, a good agreement is demonstrated between the model prediction and test results.

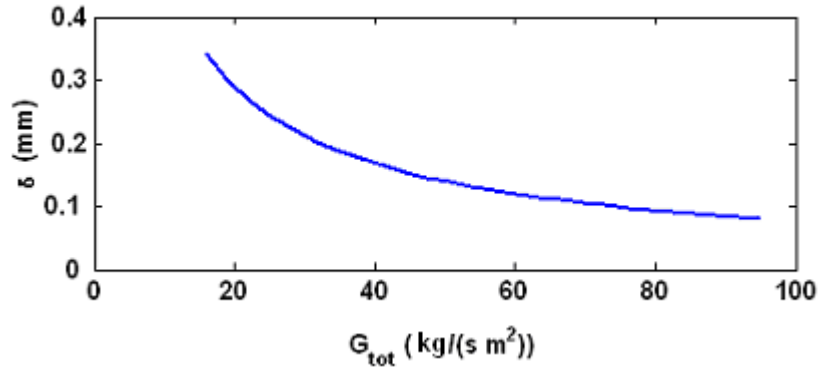

Figure 6: Liquid layer thickness predicted by the model

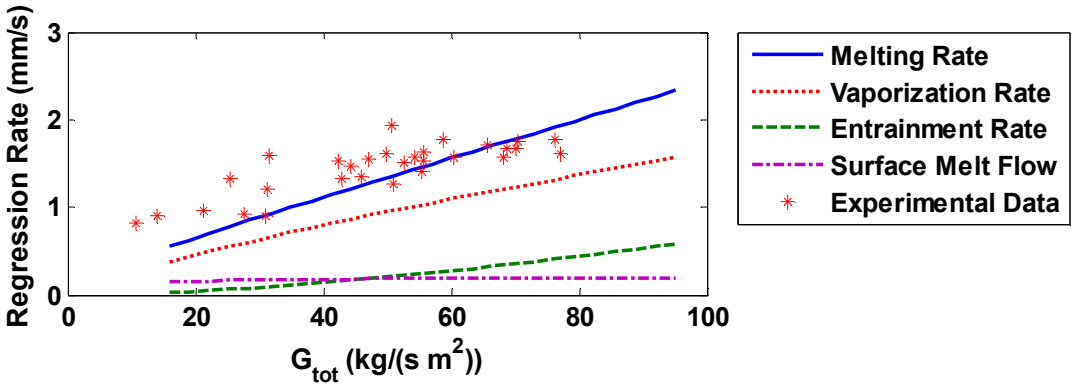

Figure 7: Regression rate mechanisms predicted by the model and related to the solid fuel density and corresponding experimental data (overall regression rate=melting rate).

The behaviour of the different mechanisms of regression rate and thickness of the liquid layer along the combustion chamber at a given time was also examined.
To calculations were made using mass conservation equation in control volume described in Figure 5.

$$\dot{m}_{l_{x+dx}} - \dot{m}_{l_x} = \dot{m}_m - \dot{m}_v - \dot{m}_{ent} = \pi d\ dx\left(\rho_s \dot{r}_m - \rho_l\left(\dot{r}_v + \dot{r}_{ent}\right)\right) \qquad \textbf{(19)}$$

where the melt flow rate at a distance x from the leading edge of the grain is:

$$\dot{m}_{l_x} = \left(\pi d\,\delta\rho_l\, u_i/2\right)_x \qquad \textbf{(20)}$$

The thickness of the melt layer changes along the grain and liquid flow average velocity was calculated from equation (11). Regression rate mechanisms were calculated from heat transfer balances as described above.
Figure 8 presents the relative contribution of each mechanism to overall regression rate (equal to melting rate). Figure 9 presents the change in molten layer thickness along the grain.

It can be observed that melting regression rate reaches a minimum value relatively close to the leading edge and later increases along the grain. The same trend of the overall regression rate was observed by Gariani at al. [14] and Chiaverini at al. [15] for the non liquefying fuels.

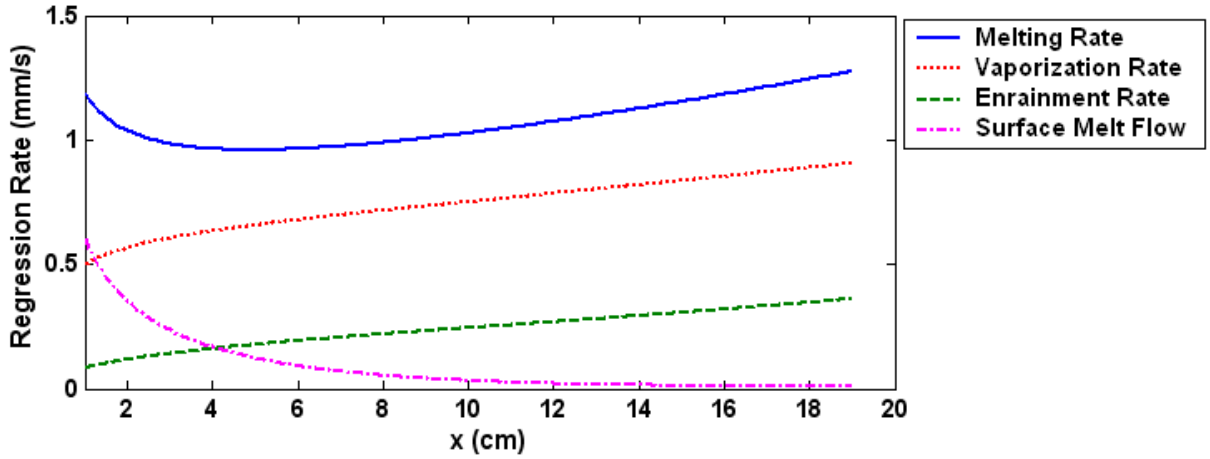

Figure 8: Regression rate contributions of the different mechanisms along the fuel grain for a total mass flux of $45\ kg/\left(s\ \ m^2\right)$ (melting rate represents the overall fuel regression rate)

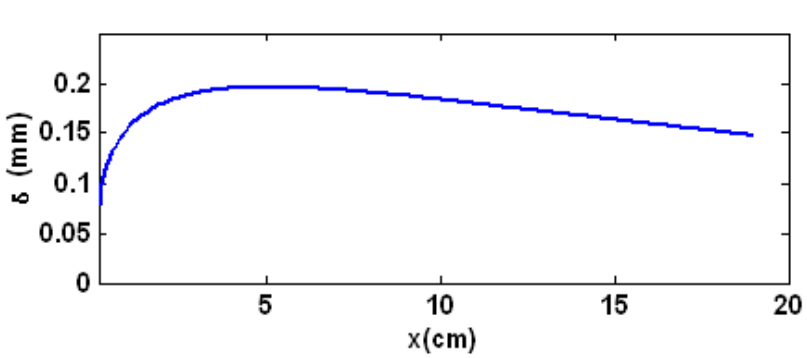

Figure 9: Prediction of liquid layer thickness along the fuel grain for a total mass flux of 45 $kg/\left(s\ \ m^2\right)$

Total mass consumption by each mechanism in combustion was calculated. It was found that 67% of the molten liquid is vaporized, 21% enters the flow by the entrainment mechanism and 11% reaches the end of the combustion chamber as flowing liquid layer. Model predicts that for a total mass flux of $45\ kg/\left(s\ \ m^2\right)$, an overall molten mass of about 5 grams should leave the combustion chamber by flowing along the surface (at the melt layer) during a 5 second firing test. It is of the same order of the amount of molten material accumulated in the after burner in actual test, indicating the significance of this mass transfer mechanism in liquefying fuels.

4. Conclusions

Based on results presented in this work, paraffin may be a good solution for burning rate enhancement in hybrid engines.

Model predictions of regression rate of a liquefying fuel yield fair agreement with the test data. The very low heat of vaporization of paraffin results in a significant contribution of the vaporization rate to the overall regression rate, more than the entrainment mechanism in the range tested.

A mechanism of liquid layer flow along the fuel surface has been added in the present model. It is shown that the mass transfer by this mechanism is of the same order as mass loss by vaporization and entrainment and, hence, should not be neglected.

The behaviour of the fuel regression rate and the contributions of the different mass loss mechanisms along the fuel grain have been calculated. About 11% of the fuel melted during the combustion has been predicted to leave the combustion chamber by flowing on the surface of the fuel grain. Test revealed that this amount is of the order of the mass of molten fuel accumulated in the aft mixing chamber, indicating the significance of this mass transfer mechanism in liquefying fuels.

One may note that some fuel droplets may leave the motor unburned. It is indicated by the large exhaust flame observed in the firing tests compared to combustion of polymeric fuels. The effect on the overall combustion efficiency has not been substantial.

This article has concentrated on the combustion phenomena and has not dealt with paraffin mechanical properties which are inferior to those of polymeric fuels.

References

[1] Altman, A. and Holzman, A. 2007. Overview and history of hybrid rocket propulsion. In: M. J. Chiaverini and K.K Kuo, Eds., Fundamentals of Hybrid Rocket Combustion and Propulsion., Progress in Astronautics and Aeronautics, AIAA, Reston, VA, Vol. 218: 1-36.

[2] Karabeyoglu, M.A., Cantwell, B.J. and Altman, D. 2001. Development and testing of paraffin-based hybrid rocket fuels. AIAA/SAE/ASME/ASEE, 37th Joint Propulsion Conference and Exhibit, AIAA-2001-4503.

[3] Karabeyoglu, M.A., Altman, D. and Cantwell, B.J. 2002. Combustion of liquefying hybrid propellants: Part 1, General theory. In: Journal of Propulsion and Power. Vol. 18, No. 3: 610-620.

[4] Karabeyoglu, M.A. and Cantwell, B.J. 2002. Combustion of liquefying hybrid propellants: Part 2, Stability of liquid films. In: Journal of Propulsion and Power. Vol. 18, No. 3: 621-630.

[5] Karabeyoglu, A., Zilliac, G., Cantwell, B.J., DeZilwa, S. and Castellucci, P. 2004. Scale-up tests of high regression rate paraffin-based hybrid rocket fuels. In: Journal of Propulsion and Power, Vol. 20, No. 6: 1037-1045.

[6] Karabeyoglu, A., Cantwell, B. J. and Stevens, J. 2005. Evaluation of homologus series of normal-alkanes as hybrid rocket fuel, AIAA/SAE/ASME/ASEE. 41th Joint Propulsion Conference, AIAA-2005-3908.

[7] Gany, A. and Lazarev, A. 2007. Fundamentals and new trends in hybrid propulsion. 6th High Energy Materials Conference and Exhibit (HEMCE-07), Chennai, India

[8] Sutton, G. 1992. Rocket propulsion elements. 6 ed., New-York: Wiley-Interscience: 512-513.

[9] Marxman, G. and Gilbert, M. 1963. Turbulent boundary layer combustion in the hybrid rocket, The Combustion Institute, 9th Symposium (International) on combustion: 1337-1349

[10] Marxman, G. A., Wooldridge, C. E., and Muzzy, R.J. 1964. Fundamentals of hybrid boundary combustion, heterogeneous combustion. Progress in Astronautics and Aeronautics, Vol.15, New-York: Academic Press: 485-522.

[11] Marxman, G. 1965. Combustion in the turbulent boundary layer on a vaporizing surface, The Combustion Institute, 10th Symposium (International) on combustion: 1337-1349.

[12] Gany, A., and Caveny, L.H. 1982. Mechanism of chemical and physical gas-metal interactions in very high shearing regimes. The Combustion Institute. 19th Symposium (International) on combustion: 731-740.

[13] Weinstein, A., Gany A. 2009. Investigation of paraffin-based fuels in hybrid combustors. Eighth International Symposium on Special Topics in Chemical Propulsion (8-ISICP). Cape Town. South Africa.

[14] Gariani, G., Maggi, F., and Galfetti, L. 2011. Numerical simulation of HTPB combustion in a 2D hybrid slab combustor , In: Acta Astronautica (2011), doi:10.1016/j.actaastro.2011.03.015.

[15] Chiaverini, M.J., Serin, N., Jhonson, D.K., Lu, Y., Kuo, K.K., and Risha, G.A. 2000. Regression rate behavior of hybrid rocket solid fuels. In: Journal of Propulsion and Power Vol. 16, No. 1: 125–132.